COMPARATIVE ANALYSIS OF EXPERIMENTAL AND NUMERICAL SIMULATION OF TWO-PHASE FLOW IN A NARROW RECTANGULAR DUCT USING OPENFOAM

Phakhinai Samor, Narakhan Khunsrimek, Autthasith Panyopas, Somboon Rassame

Department of Nuclear Engineering, Faculty of Engineering Chulalongkorn University, Wangmai, Patumwan, Bangkok 10330, Thailand

ABSTRACT

Bubbly flow represents a fundamental two-phase flow regime characterized by the dispersion of gas bubbles within a continuous liquid phase. This regime plays a critical role in heat transfer and coolant performance, particularly within confined geometries such as narrow vertical channels commonly found in nuclear reactor systems. In this study, the open-source computational fluid dynamics (CFD) software, OpenFOAM version 12 is employed to simulate vertical air-water two-phase flow within a rectangular duct measuring 10 mm × 200 mm × 2.95 m. The simulation replicates two experimental cases reported by Liu (2008), which differ in gas injection rates while maintaining a constant liquid flow rate. The multiphaseEulerFoam solver is applied with interfacial force models that include drag, lift, wall lubrication, and virtual mass. Additionally, the two-group Interfacial Area Transport Equation (IATE) model is used to represent bubble coalescence and breakup mechanisms. Key flow parameters, including the Sauter mean diameter, void fraction, bubble velocity, and interfacial area concentration, are evaluated at six axial locations. The simulation results are validated against experimental data at z/D_{H} = 34.8, 88.2, and 141.7 through graphical trend comparisons and relative error analysis. The findings indicate that the model performs well in the low gas flow case, while greater discrepancies are observed in the high gas flow case, particularly in the Sauter mean diameter and interfacial area concentration. These differences highlight limitations in accurately predicting bubble coalescence and spatial distribution under more complex flow conditions.

Keywords: OpenFOAM, Two-phase flow, Bubbly flow, IATE model, Interfacial force

I. INTRODUCTION

Bubbly flow is one of the two fundamental flow regimes involving two phases, characterized by the dispersion of small gas bubbles within a continuous liquid phase without the bubbles coalescing to form larger clusters. It significantly affects shear stress, momentum exchange, and heat transfer and is commonly observed in thermal and energy systems such as nuclear reactor cooling, heat exchangers, and chemical processing units [1,2]. An accurate understanding of bubbly flow behavior is essential for ensuring system stability and improving performance, particularly in narrow channels where bubble distribution and interfacial interactions are greatly affected by confinement [1,3]. In marine engineering applications, where plate-type fuel elements are commonly used, narrow duct channels are often subjected to external ship motions such as rolling. Jin et al. [4] have shown that rolling motion can significantly influence two-phase flow characteristics, leading to oscillatory pressure drops and intensified interfacial interactions due to time-dependent inertial forces. Although the present work focuses on stationary vertical bubbly flow, these dynamic effects may be of interest for future investigations on flow stability in marine reactor systems.

Computational Fluid Dynamics (CFD) has become a powerful tool for analyzing complex flow phenomena such as bubbly flow [5]. However, commercial CFD software packages such as ANSYS Fluent and STAR-CCM+ often have high licensing costs and restricted access, which poses challenges for research groups and academic use, particularly at the student level [5]. OpenFOAM, an open-source CFD software package, is a popular alternative due to its free accessibility, high flexibility, and ability to simulate complex multiphase flows [6]. OpenFOAM supports a wide range of physical models, including multiphase flows, heat transfer, reacting flows, and turbulent phenomena [5]. It has been applied in a variety of academic and industrial contexts, including bubble columns, injectors, pipe flow, and narrow-duct simulations [2]. Furthermore, its use has been documented in the fields of power generation and nuclear engineering [6], demonstrating its relevance to high-stakes systems. In this study, OpenFOAM is used to simulate a case based on an experiment conducted by Liu et al. [1] in a vertical narrow

duct that mimics conditions in reactor cooling channels. This reinforces the relevance of this study to nuclear engineering applications. Although several studies have simulated bubbly flows using OpenFOAM, no prior work has been found that directly reproduces the experimental conditions of Liu while incorporating the two-group Interfacial Area Transport Equation (IATE) model. Liu's dataset provides high-quality benchmark data that is well-suited for validating CFD models. This study, therefore, aims to address this research gap by implementing a detailed Eulerian-Eulerian two-fluid CFD simulation in OpenFOAM. The simulation incorporates interfacial force models, including drag, lift, wall lubrication, and turbulent dispersion, in addition to the two-group IATE model.

This study aims to simulate bubbly two-phase flow under conditions similar to those in the experiment conducted by Liu (2008), using OpenFOAM version 12. The simulation replicates the air-water flow in a vertical narrow rectangular duct with dimensions of 10 mm × 200 mm × 2.95 m. While Liu's experiment collected data only at z/D_H = 34.8, 88.2, and 141.7, the present study extends the analysis to all six axial positions to enable a more detailed evaluation of bubble behavior along the vertical channel. Two gas injection cases are considered, and the simulation results are compared with Liu's experimental data. Key parameters analyzed include the Sauter mean diameter, void fraction, bubble velocity, and interfacial area concentration (IAC). The aim is to evaluate the accuracy of the CFD model based on the two-group Interfacial Area Transport Equation (IATE), and to demonstrate the applicability of OpenFOAM for detailed investigations of bubbly flow behavior.

II. THEORETICAL BACKGROUND

II.A. Two-Fluid Model

The two-fluid model is a mathematical framework employed to describe two-phase flow by treating each phase, such as gas and liquid, as a continuous medium governed by its own conservation equations for mass, momentum, and energy [7]. This facilitates the lucid modeling of interfacial phenomena, including drag, lift, wall lubrication, turbulent dispersion, virtual mass, and heat transfer [7]. To derive practical macroscopic field equations, Eulerian averaging methods are commonly applied, making the model suitable for engineering-scale problems such as transient flow and complex reactor geometries. In practice, the model can be formulated in two main approaches: the Euler-Lagrange method and the Euler-Euler method. The Euler-Lagrange approach is characterized by its ability to track dispersed-phase particles individually. In contrast, the Euler-Euler approach, which is the method employed in this study, treats both phases as interpenetrating continua. The volume fraction is employed to denote the proportion of each phase, and separate conservation equations are solved for each. Assuming negligible mass transfer between phases, the governing equations employed in this study consist of the continuity and momentum conservation equations, shown respectively in Equations (1) and (2) [6].

$$\frac{\partial(\alpha_k \rho_k)}{\partial t} + \nabla \cdot (\alpha_k \rho_k \vec{u}_k) = 0 \ , \tag{1}$$

$$\frac{\partial(\alpha_k \rho_k \vec{u}_k)}{\partial t} + \nabla \cdot (\alpha_k \rho_k \vec{u}_k \vec{u}_k) = -\alpha_k \nabla p + \alpha_k \rho_k \vec{g} + \nabla \cdot (\alpha_k \tau_k) + \overrightarrow{M}_{I \to k} \ , \tag{2}$$

where α_k is the volume fraction of the phase k [-], ρ_k is the density [kg/m^3], $\vec{u}_k$ is the velocity [m/s], p is the pressure [Pa], $\vec{g}$ is the gravitational acceleration [m/s^2], τ_k is the viscous stress tensor [Pa], and $\overrightarrow{M}_{I \to k}$ is the interfacial momentum transfer from phase I to phase k [N/m^3]. The two-fluid model serves as a fundamental approach for simulating multiphase flow, particularly in cases requiring high accuracy and clear phase separation.

II.B. Interfacial Force

Interfacial momentum transfer or interfacial forces exert a significant influence on the motion, distribution, and interaction of gas bubbles in two-phase flows. In vertical systems, the effects of these ions are of particular significance, as wall interactions influence the lateral migration and arrangement of bubbles. These forces have been shown to affect flow stability, phase distribution, and energy transport mechanisms [7]. In this study, five interfacial forces are considered, including drag, lift, wall lubrication, turbulent dispersion, and virtual mass forces. The total interfacial momentum exchange between phases is represented by Equation (3), which combines these individual components.

$$\overrightarrow{M}_{I \to k} = \overrightarrow{M}_{f \to g} = -\overrightarrow{M}_{g \to f} = \overrightarrow{F}_{D,f \to g} + \overrightarrow{F}_{L,f \to g} + \overrightarrow{F}_{TD,f \to g} + \overrightarrow{F}_{VM,f \to g} + \overrightarrow{F}_{WL,f \to g} \ , \tag{3}$$

Where $\overrightarrow{F}_{D,f\to g}$ is the drag force [N/m^3] resisting relative motion between phases, $\overrightarrow{F}_{L,f\to g}$ is the lift force [N/m^3] resulting from velocity gradients that cause lateral migration of bubbles, $\overrightarrow{F}_{TD,f\to g}$ is the turbulent dispersion force [N/m^3] that redistributes bubbles due to turbulence, $\overrightarrow{F}_{VM,f\to g}$ is the virtual mass force [N/m^3] arising from the acceleration of bubbles relative to the liquid phase, and $\overrightarrow{F}_{WL,f\to g}$ is the wall lubrication force [N/m^3] that repels bubbles from walls and reduces near-wall accumulation [7].

II.C. Interfacial Area Concentration and Transport Equation (IATE)

In gas-liquid two-phase flow, particularly under bubbly flow conditions, the dynamic behavior of the interfacial structure significantly affects the transport of mass, momentum, and energy. The interfacial area concentration a_i, defined as the total interfacial surface area per unit mixture volume, is a key parameter for characterizing gas-liquid interaction and predicting two-phase behavior [8]. The interfacial area is subject to continuous changes due to bubble coalescence and breakup, which must be considered for accurate modeling of the flow structure [8]. To account for these variations, the one-group Interfacial Area Transport Equation (IATE) is employed to describe the temporal and spatial evolution of a_i, incorporating source and sink terms representing physical bubble interactions [8]. Among these mechanisms, bubble breakup caused by turbulent eddies is dominant in bubbly flows, and the corresponding source term is given in Equation (4)

$$\frac{\partial a_i}{\partial t} + \nabla(a_i \vec{v}_i) \cong \frac{2}{3}\left(\frac{a_i}{\alpha}\right)\left(\frac{\partial \alpha}{\partial t} + \nabla \cdot \left(\alpha \vec{u}_g\right)\right) + \frac{1}{3\psi}\left(\frac{\alpha}{a_i}\right)^2 \sum_j R_j \tag{4}$$

Where a_i is the interfacial area concentration [m^{-1}], $\vec{v}_i$ is the interfacial velocity [m/s], α is the void fraction [-], $\vec{u}_g$ is the gas velocity [m/s], and R_j represents the source terms due to bubble interaction mechanisms such as coalescence and breakup. For spherical or near-spherical bubbles [m^{-3}/s^{-1}], the bubble shape factor ψ is taken as $1/(36\pi)$. Besides, $\vec{v}_i$ often approximated by the gas velocity $\vec{u}_g$

II.D. Turbulence Modeling

Turbulence plays a central role in the behavior of bubbly two-phase flows by influencing momentum exchange, phase dispersion, and interfacial interactions. In this study, turbulence in the continuous liquid phase is modeled using the Shear Stress Transport (SST) $k-\omega$ model [9], which combines the robustness of the $k-\varepsilon$ model in the freestream with the near-wall accuracy of the $k-\omega$ formulation through a blending function. The transport equation for the turbulent kinetic energy k is given in Equation (5), and the equation for the specific dissipation rate ω is given in Equation (6)

$$\frac{\partial(\alpha_f \rho_f k_f)}{\partial t} + \nabla \cdot (\alpha_f \rho_f \vec{u}_f k_f) = \nabla \cdot \left[\alpha_f \left(\mu_f{}^{mol} + \frac{\mu_f{}^{turb}}{\sigma_{k3}}\right)\nabla k_f\right] + \alpha_f \rho_f - \acute{\beta} \alpha_f \rho_f k_f \omega_f + S_k \tag{5}$$

$$\frac{\partial(\alpha_f \rho_f \omega_f)}{\partial t} + \nabla \cdot (\alpha_f \rho_f \vec{u}_f \omega_f) = \nabla \cdot \left[\alpha_f \left(\mu_f{}^{mol} + \frac{\mu_f{}^{turb}}{\sigma_{\omega 3}}\right)\nabla \omega_f\right] + (1-F_1) 2\alpha_f \rho_f \frac{\nabla k_f \nabla \omega_f}{\sigma_{\omega 2} \omega_f} + a_3 \alpha_f \frac{\omega_f}{k_f} P_k - \beta_3 \alpha_f \rho_f k_f {\omega_f}^2 + S_\omega \tag{6}$$

In order to capture the additional turbulence generated by dispersed bubbles, the standard SST model is extended using a bubble-induced viscosity term based on Sato's formulation [10]. The modified turbulent viscosity is expressed in Equation (7).

$$\mu_L{}^{turb} = \frac{a_1 \rho_f k_f}{\max(a_1 \omega_f, F_2 \sqrt{S^2})} + (1 - e^{-\frac{y^+}{16}})^2 \cdot C_{\mu b} \cdot d \cdot \alpha_f \cdot \left|\vec{u}_g - \vec{u}_f\right| \tag{7}$$

In these equations, α_f is the volume fraction [-] of the liquid phase, ρ_f is the liquid density [kg/m^3], $\vec{u}_f$ and $\vec{u}_g$ are the velocity [m/s^2] of the liquid and gas phases, respectively, k_f and ω_f are the turbulent kinetic energy [m^2/s^2] and specific dissipation rate [s^{-1}] of the liquid phase. $\mu_f{}^{mol}$ and $\mu_f{}^{turb}$ denote the molecular and turbulent viscosities $[Pa \cdot s]$ of the liquid phase. P_k is the turbulence production term due to shear, while S_k and S_ω represent additional source terms that account for bubble-induced turbulence. In the eddy viscosity expression, d is the bubble diameter [m], $C_{\mu b}$ is the empirical coefficient for bubble-induced turbulence, and y^+ is the dimensionless wall distance. The strain-rate magnitude is represented by S, and the

functions $F_1$and F_2 are first and second blending functions used in the SST formulation. The constants σ_{k3} ,$\sigma_{\omega 3}$, $\sigma_{\omega 2}$, $\acute{\beta}$, β_3, a_1, a_3 are model coefficients from the standard SST formulation. This set of equations provides a more accurate representation of near-wall turbulence in confined bubbly flows by including bubble-induced effects.

III. METHODOLOGY

III.A. Initial and Boundary Conditions

The computational domain was defined as a narrow rectangular channel with a width of 10 mm, a length of 200 mm, and a height of 2950 mm, consistent with the experimental setup of Liu et al. [1]. To capture spatially resolved data, surface probes were installed at six vertical positions along the z-axis (z/D_H) = 8.0, 34.8, 61.5, 88.2, 115.0, and 141.7) where D_H = 19.05 mm. These probes were used to monitor pressure, velocity, void fraction, interfacial area concentration, Sauter mean diameter (D_{sm}), and maximum bubble diameter. The results from these positions were later used for comparison with experimental data and model evaluation. These configurations are illustrated in Fig. 1.

In accordance with the study conducted by Liu et al. [1], which examined vertical two-phase air-water flow under conditions of non-uniform bubble distribution, the bubble structures were classified into two categories: bubbly flow and slug flow. The present study selected two cases that fall within the bubbly flow regime to investigate bubble behavior in water under high-turbulence conditions. As shown in Table I, the superficial liquid velocity (j_f) was fixed at 2.531 m/s for both cases, while the superficial gas velocity (j_g) was 0.090 m/s for Case A and 0.305 m/s for Case B. Since Liu et al. [1] did not report the void fraction at the inlet, the void fractions at z/D_H = 34.8 were adopted instead, with values of 0.029 for Case A and 0.086 for Case B. These were considered the most representative values for initializing the phase volume fraction (α) in the simulation. In addition, the fluid temperature was maintained at a constant 26.8°C throughout the entire simulation domain. The aforementioned values were then used to calculate the turbulent kinetic energy (k), specific dissipation rate (ω), and turbulent viscosity (μ). These turbulence quantities, along with the flow velocity (v) and the void fraction (α), were employed as the initial conditions for the numerical model.

The initial bubble diameters were set at 1.96 mm for Case A and 2.54 mm for Case B, based on calibration to match Liu's experimental results at z/D_H = 34.8. The definition of the boundary conditions was informed by the study conducted by Liao et al. [1], which also employed the OpenFOAM software to simulate bubbly flow. The two-phase system consisted of air and water. The air phase employed the two-group Interfacial Area Transport Equation (IATE) model from Ishii et al. (2001), with parameters selected specifically for bubbly flow. Water was designated as the continuous phase. The interfacial forces under consideration encompassed drag, lift, wall lubrication, turbulent dispersion, and virtual mass. The fluid properties were defined according to the same thermal conditions: water was defined with constant density and viscosity, while air was modelled with variable density. The turbulence model employed for the water phase was the k-omega SST Sato model, while the air phase was treated as laminar. The computational mesh used was a multigrading structured mesh consisting of 25 × 1 × 150 cells, as illustrated in Fig. 1. This configuration provided increased resolution near the channel walls, where shear and interfacial forces significantly influenced bubble behavior. The mesh type was selected to achieve a balance between computational efficiency, numerical stability, and solution accuracy. The simulation was performed for a total duration of 60 seconds.

III.B. OpenFOAM Software

OpenFOAM is a software solution for computational fluid dynamics (CFD) that is characterized by its open-source nature. It is utilized for the purpose of simulating complex fluid systems. The present study utilized the multiphaseEulerFoam solver, which is based on the Euler-Euler model, for the purpose of analyzing two-phase flows. The fundamental equations solved included the continuity and momentum equations. Moreover, supplementary models were incorporated to account for interfacial phenomena and turbulence characteristics: the Interfacial Area Transport Equation (IATE) for interfacial surface area prediction and the k-omega SST Sato model for modelling turbulence in the water phase.

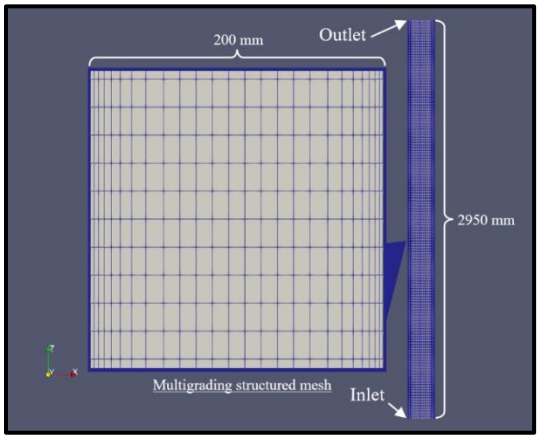

FIGURE 1. Computational domain geometry and multigrading mesh used in the OpenFOAM simulation.

TABLE I. Initial Conditions for Case A and Case B

Case	j_f [m/s]	j_g [m/s]
A	2.531	0.090
B	2.531	0.305

III.B. OpenFOAM Software

OpenFOAM is a software solution for computational fluid dynamics (CFD) that is characterized by its open-source nature. It is utilized for the purpose of simulating complex fluid systems. The present study utilized the multiphaseEulerFoam solver, which is based on the Euler-Euler model, for the purpose of analyzing two-phase flows. The fundamental equations solved included the continuity and momentum equations. Moreover, supplementary models were incorporated to account for interfacial phenomena and turbulence characteristics: the Interfacial Area Transport Equation (IATE) for interfacial surface area prediction and the k-omega SST Sato model for modelling turbulence in the water phase.

III.C. Calculation Process

With regard to the input part, the initial conditions were defined for the following parameters: velocity (v), phase volume fraction (α), turbulent kinetic energy (k), specific dissipation rate (ω), turbulent viscosity (μ), and temperature (T). The initial diameters of the bubbles, as well as the physical properties of both air and water, were assigned. Furthermore, parameter ranges were established for interfacial forces, turbulence models, and simulation controls (such as duration and output frequency). As for the pre-processing part, a multigrading structured mesh with 25 × 1 × 150 cells was created. This mesh increased the resolution near the wall region, where shear and interfacial forces have significant effects on the behavior of bubbles. The mesh configuration was influenced by the prior input values, and a validation process was conducted to confirm the accuracy of the mesh and input settings.

With regard to the calculation element, the solver performed numerical integration of the continuity and momentum equations at each time step. Additional calculations were carried out using the IATE model to estimate interfacial area and the k-omega SST Sato model to represent turbulence effects in the continuous phase. The simulation was executed over a total time period of 60 seconds. A comprehensive set of physical parameters was meticulously measured at six predetermined axial locations along the vertical channel. These parameters encompassed critical variables such as pressure, velocity, void fraction, interfacial area concentration, and bubble size. The measurements were obtained from surface probes, ensuring the collection of reliable and representative data. The void fraction, interfacial area concentration, and bubble size were processed using area averaging, whereas velocity was averaged using the area-weighted method. The mean values thus obtained were then utilized to calculate the relative error percentage (RE%) for model verification by comparing the simulation outcomes at three specific axial positions (z/D_H = 34.8, 88.2, and 141.7) against the experimental data in order to assess the model's accuracy and performance.

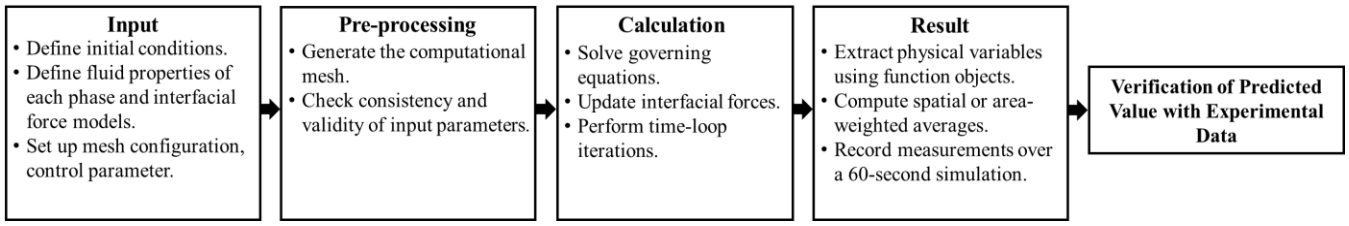

FIGURE 2. Workflow of the CFD Simulation Process in OpenFOAM

IV. RESULTS AND DISCUSSION

To assess the predictive performance of the computational fluid dynamics (CFD) model for vertical air–water two-phase flow, simulation results were benchmarked against experimental data obtained by Liu at three axial positions corresponding to dimensionless heights (z/D_H) of 34.8, 88.2, and 141.7. Four key parameters were evaluated, namely the Sauter mean diameter, void fraction, bubble velocity, and interfacial area concentration, which are presented in Figs. 3(a), 3(b), 3(c), and 3(d), respectively. Each plot illustrates the variation of the corresponding parameter along the dimensionless vertical axis (z/D_H). In the graphs, solid lines denote simulation results, while dashed lines represent experimental measurements. Case A is plotted in black, whereas Case B is represented in red to distinguish between the two test conditions.

IV.A. Sauter Diameter

As demonstrated in Fig. 3(a), the graph of Case A demonstrates a steadily increasing trend along the axial direction and remains closely aligned with the experimental data at all measurement points. Conversely, Case B demonstrates considerably elevated values in comparison to the experimental outcomes, particularly within the upper segment of the channel, where intensified bubble coalescence results in an overestimation of the mean bubble size. As illustrated in Table II, the simulation in Case A generates minimal relative errors of 0.30%, -0.83%, and -3.61% at z/D_H = 34.8, 88.2, and 141.7, respectively. Conversely, Case B exhibited substantially higher deviations, with relative errors reaching 38.57% and 44.51% at z/D_H = 88.2, and 141.7, respectively. These findings suggest that the current model is deficient in its capacity to adequately capture the phenomenon of bubble coalescence under conditions of elevated gas flow.

IV.B. Void Fraction

As shown in Fig. 3(b), both cases exhibit an increasing trend in void fraction along the vertical direction, which corresponds to the upward motion and accumulation of bubbles in the duct. In Case A, the simulation trend generally follows experimental data, but noticeable deviations remain at z/D_H = 34.8 and 141.7, with only z/D_H = 88.2 showing a relatively close match. In Case B, the void fraction is consistently overpredicted along the height, but the deviation appears to decrease with increasing axial length. As illustrated in Table II, the relative errors for Case A are 14.39%, 8.47%, and 17.57% at z/D_H = 34.8, 88.2, and 141.7, respectively, while for Case B, the errors decreased progressively from 22.28% to 17.89% and 11.60%. This finding indicates that the model's capacity to predict the void fraction in Case B is likely to undergo enhancement as the process progresses, a phenomenon that may be attributed to the escalating bubble dispersion over time.

IV.C. Velocity

As shown in Fig. 3(c), the graphs for both Case A and Case B remain relatively constant along the axial direction, reflecting the uniform upward motion of bubbles throughout the channel. In Case A, the simulated bubble velocity tends to exceed the experimental measurements at all positions to a minor extent. Table II shows relative errors of 17.11%, 15.26%, and 10.53% at z/D_H = 34.8, 88.2, and 141.7, respectively. A similar trend is observed in Case B, where the simulation also overpredicts the velocity with relative errors of 14.79%, 15.64%, and 13.37% at the corresponding positions. These results suggest that the model successfully captures the overall velocity trend, but moderate quantitative deviations remain, generally within the range of 10 - 17%.

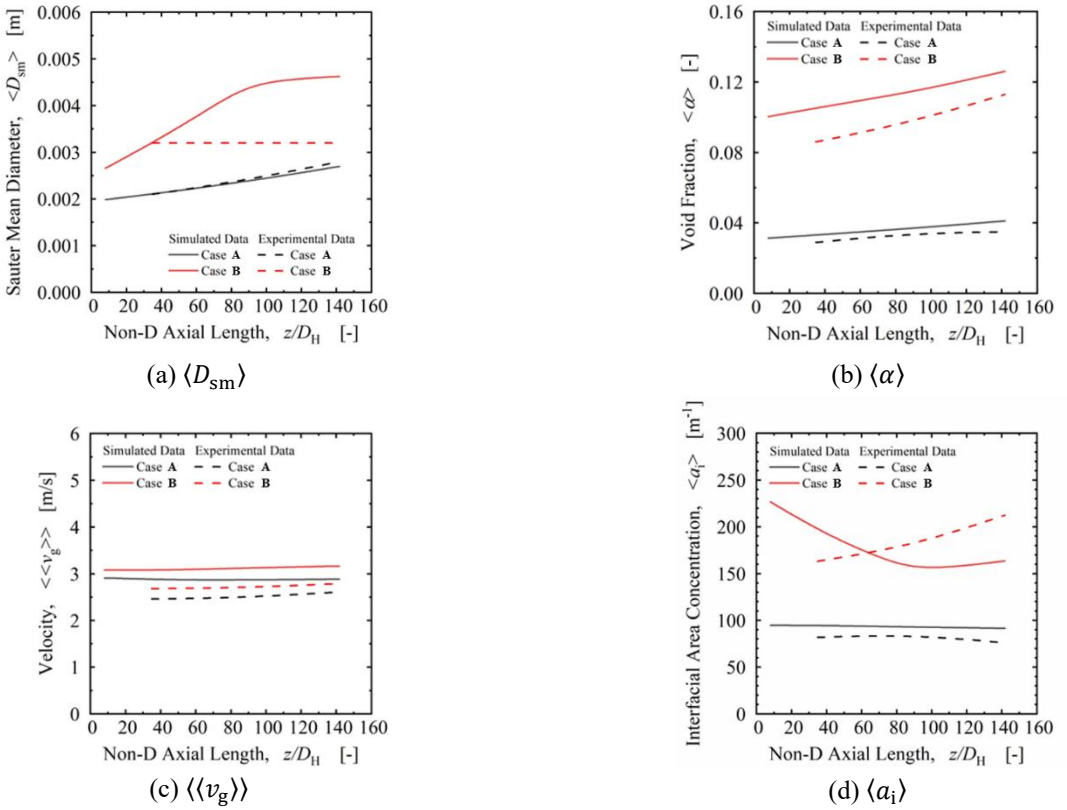

FIGURE 3. Comparison between Experimental data and Simulation data (a) $\langle D_{sm} \rangle$, (b) $\langle \alpha \rangle$, (c) $\langle \langle v_g \rangle \rangle$, and (d) $\langle a_i \rangle$

TABLE II. Relative Error Percentage

Cases	z/D_H	Percent of $\langle D_{sm} \rangle$ [%]	Percent of $\langle \alpha \rangle$ [%]	Percent of $\langle \langle v_g \rangle \rangle$ [%]	Percent of $\langle a_i \rangle$ [%]
A	34.8	0.30	14.39	17.11	15.52
	88.2	-0.83	8.47	15.26	9.51
	141.7	-3.61	17.57	10.53	20.37
B	34.8	0.04	22.28	14.79	20.70
	88.2	38.57	17.89	15.64	-13.70
	141.7	44.51	11.60	13.37	-23.00

IV.D. Interfacial Area Concentration (IAC)

As demonstrated in Fig. 3(d), both cases exhibit a decreasing trend in interfacial area concentration along the vertical axis, which reflects bubble coalescence leading to a reduction in total gas-liquid interface. In Case A, the simulation trend manifests as relatively flat, exhibiting reasonable congruence with the experimental data, though deviations emerge at z/D_H = 34.8 and 141.7. As illustrated in Table II., the relative errors for Case A are 15.52%, 9.51%, and 20.37% at z/D_H = 34.8, 88.2, and 141.7, respectively, indicating moderate agreement. In Case B, the simulation overpredicts the interfacial area at z/D_H = 34.8 with a relative error of 20.70%, but then increasingly underpredicts it at downstream locations, with errors of -13.70% and -23.00% at z/D_H = 88.2 and 141.7, respectively. This alteration in deviation direction indicates that, while the model does capture the decreasing trend caused by coalescence, it still lacks the necessary accuracy to adequately represent interfacial area dynamics under conditions of high gas flow, possibly due to intensified coalescence and vertical redistribution of bubbles.

V. CONCLUSIONS

The two-phase flow of bubbles in narrow vertical channels is of particular importance in determining heat transfer performance and system stability, particularly in the field of nuclear engineering. Although CFD is widely used to simulate such flows, commercial software packages present limitations in terms of cost and accessibility. OpenFOAM, an open-source and highly flexible CFD platform, offers an effective alternative for modelling complex multiphase systems. Although prior studies have employed OpenFOAM to simulate bubbly flow, only a limited number have focused specifically on turbulent bubbly flow in narrow rectangular channels. The present study aims to address this research gap by employing OpenFOAM with a two-group Interfacial Area Transport Equation (IATE) model and comprehensive interfacial force modelling to replicate Liu's experiment in a narrow rectangular duct. The key aspects of this study can be summarized as follows:

- The initial simulation parameters were defined according to the experimental setup of Cases A and B. The gas flow rates exhibited by these cases are subject to variation, with B demonstrating a higher rate in comparison to A. However, the liquid flow rate was maintained at a constant level throughout the experimentation. The simulations were conducted within a narrow vertical duct measuring 10 mm × 200 mm × 2.95 m. The OpenFOAM version 12 software was utilized for the execution of simulations, with the multiphaseEulerFoam solver employed to facilitate the computations. This solver incorporates interfacial force models, encompassing drag, lift, wall lubrication, and virtual mass. Furthermore, the two-group Interfacial Area Transport Equation (IATE) model was implemented in order to account for bubble coalescence and breakup.

- Six axial measurement positions were established along the duct's height. Surface probes were utilized to obtain area-averaged values of Sauter mean diameter $\langle D_{\mathrm{sm}} \rangle$, void fraction $\langle \alpha \rangle$, and interfacial area concentration $\langle a_{\mathrm{i}} \rangle$, while void-weighted averaging was applied to calculate the gas phase velocity $\langle \langle v_{\mathrm{g}} \rangle \rangle$. The simulation results were then compared with the experimental data set collected by Liu at z/D_{H} = 34.8, 88.2, and 141.7. The evaluation process entailed graphical comparisons of trends and quantitative assessments of relative errors (RE) for all four parameters: $\langle D_{\mathrm{sm}} \rangle$, $\langle \alpha \rangle$, $\langle \langle v_{\mathrm{g}} \rangle \rangle$, and $\langle a_{\mathrm{i}} \rangle$.

- Case A (low gas flow rate) demonstrated a strong correlation with the experimental data, particularly in $\langle D_{\mathrm{sm}} \rangle$ and $\langle \langle v_{\mathrm{g}} \rangle \rangle$, where the trends and relative errors remained within acceptable limits. Case B (high gas flow rate) exhibited greater deviation, especially in $\langle D_{\mathrm{sm}} \rangle$ and $\langle a_{\mathrm{i}} \rangle$, where the model failed to accurately capture the behavior of bubble coalescence. For $\langle a_{\mathrm{i}} \rangle$, the simulated values were higher than the experimental data in the lower region of the duct and lower toward the top, suggesting a shift in error direction along the vertical axis. This suggests a potential spatial inconsistency in the prediction of bubble distribution and interfacial area concentration. In conclusion, the model demonstrates reasonable predictive capability for bubbly flow behavior under low gas flow conditions. However, to improve accuracy under more complex flow regimes with higher gas injection rates, further refinement of the IATE model parameters such as the coalescence coefficient (C_{WE}), the breakup coefficient (C_{WE}), and the turbulent interaction coefficient (C_{WE}) as well as the interfacial force models is necessary.

REFERENCES

[1] Liu, Yang. "Three-dimensional interfacial area transport in gas-dispersed two-phase flow up to churn-annular flow transition." PhD diss., Purdue University, 2008.
[2] Liao, Yixiang, Kartik Upadhyay, and Fabian Schlegel. "Eulerian-Eulerian two-fluid model for laminar bubbly pipe flows: Validation of the baseline model." *Computers & Fluids* 202 (2020): 104496.
[3] Poullikkas, A. "Two phase flow performance of nuclear reactor cooling pumps." *Progress in Nuclear energy* 36, no. 2 (2000): 123-130.
[4] Jin, Guangyuan, et al. "Effect of rolling motion on transient flow resistance of two-phase flow in a narrow rectangular duct." *Annals of Nuclear Energy* 64 (2014): 135-143.
[5] Medina, Humberto, Abhinivesh Beechook, Jonathan Saul, Sophie Porter, Svetlana Aleksandrova, and Steve Benjamin. "Open source computational fluid dynamics using OpenFOAM." In *Royal Aeronautical Society, General Aviation Conference, London*. 2015.
[6] Jasak, Hrvoje. "OpenFOAM: Open source CFD in research and industry." *International journal of naval architecture and ocean engineering* 1, no. 2 (2009): 89-94.

[7] Ishii, Mamoru, and Kaichiro Mishima. "Two-fluid model and hydrodynamic constitutive relations." *Nuclear Engineering and design* 82, no. 2-3 (1984): 107-126.
[8] Wang, Xia, and Xiaodong Sun. "Three-dimensional simulations of air–water bubbly flows." *International journal of multiphase flow* 36, no. 11-12 (2010): 882-890.
[9] Menter, Florian R. "Elements of inductrial heat tranfer predictions." In *16th Brazilian Congress of Mechanical Engineering (COBEM), Uberlandia, Brazil, 2001*. 2001.
[10] Sato, Y., M. Sadatomi, and K. Sekoguchi. "Momentum and heat transfer in two-phase bubble flow—I. Theory." *International Journal of Multiphase Flow* 7, no. 2 (1981): 167-177.